

Simulating Cosmic Rays Propagating In Earth's Atmosphere

Finlo Heath
(Dated: March 28, 2020)

Abstract

Cosmic rays are a physical phenomenon that have been studied since the early twentieth century. This project aimed to use Python, an object oriented coding language, to produce an accurate simulation of cosmic rays propagating in Earth's atmosphere. The program simulates primary cosmic rays from their entry into the upper atmosphere to the point of their interaction, or until they slow to a stop due to the electronic stopping power of electrons in atmospheric molecules. Interactions can be enabled or disabled, allowing the possibility of using the program to study other physical systems where the motion of charged particles in a medium is dictated by an electronic stopping force. The program accurately simulates the motion of non-interacting charged particles in the atmosphere, producing phenomena such as exponential deceleration and the Bragg peak in kinetic energy transfer as a function of distance travelled; both of which are well documented in physical observations. Interacting cosmic ray simulations have an interaction probability proportional to the distance travelled, the mean interaction length falling on average within ± 40 m of the observed value, 700 m.

CONTENTS

I. Introduction	2
II. Theory	3
III. Design	6
A. Creating Charged Particles	6
B. Applying the Bethe Formula	6
C. Utilising Data Frames	8
D. Multiple Particles	8
E. Primary Cosmic Ray Interactions	9
F. Relativistic Adjustments	10
G. Test Functions	10
H. Final Design	10
IV. Results & Analysis	12
A. Non-Interacting Primary Cosmic Rays	12
B. Interacting Primary Cosmic Rays	14
V. Further Work	17
VI. Conclusions	18
VII. Bibliography	19
References	19
A. Calculation of Mean Density for Atmospheric Layers	20

I. INTRODUCTION

Cosmic ray physics has provided a range of scientific advancements since their discovery in August 1912 through to the modern day [1]. Their study in physics institutions across the globe maintains an integral function in both teaching and leading research, particularly at Lancaster University itself [2][3]. Cosmic rays are categorised in two ways. Primary cosmic rays originate outside of Earth's atmosphere from a variety of sources both within and outside of our solar system and galaxy [1][4]. These include our own sun, supernovae and possibly other sources such as active red dwarf stars [4]. Primary Cosmic rays are light stable nuclei; 89% are protons (hydrogen nuclei), 10% are helium nuclei and the remaining percent are heavier nuclei [1]. If primary cosmic rays are incident on the atmosphere of Earth, they may interact with atmospheric molecules and produce secondary cosmic rays; short lived, fast moving particles produced within Earth's atmosphere [1].

While physical measurements of secondary cosmic ray flux are standard in such institutions, the aim of the project detailed in this report was to use Python 3.7.3 to create a physically accurate simulation of cosmic rays propagating through Earth's atmosphere. The purpose of such a simulation is to give greater clarity on the whole journey of the cosmic rays through the atmosphere as well as to investigate how key parameters such as the energy and velocity of cosmic rays change as propagate. Of particular interest is the simulation of primary cosmic rays since physical measurements on Earth's surface are limited to observing secondary cosmic ray flux. For this reason, the simulation of primary cosmic rays served as the focus of this project. Specifically, this included applying the electronic stopping force acting on these particles due to the molecules in the atmosphere in combination with there being a variable probability that the particles will interact with these molecules. Such interactions produce short lived secondary cosmic rays which begin a particle shower through a series of decays [1].

Due to their complexity and the limited time allowed to build the simulation, secondary cosmic ray showers were not included in the model. Hence the model is limited to primary cosmic rays from the moment they enter Mesosphere, the outermost layer of the Earth's atmosphere with a significant air density [5], to the point at which they slow to a stop or have interacted with air molecules.

While the motivation of this project is certainly to produce an accurate simulation for the purpose of furthering scientific understanding of primary cosmic rays, there are physical applications of such a model. A key application of modelling protons experiencing a Bethe stopping force is in medical charged particle radiotherapy, where protons are used as an alternative to photons for radiotherapy; knowledge of proton trajectory and energy through a medium (such as human tissue) is therefore essential to ensure such applications are medically viable [6].

The following section of the report includes details on the physics supporting the model as well as the physical quantities being investigated. The Design section outlines the process of creating and improving the simulation through each of its iterations. The results are then presented along with analysis in reference to real physical observations which the model sought to replicate. Finally, suggested potential improvements and extensions to the simulation are proposed and conclusions on the project are made.

II. THEORY

As outlined in Section I, the model simulates primary cosmic rays starting from their entry into the Mesosphere. As hydrogen nuclei compose the vast majority of cosmic rays incident on the atmosphere, the model initialises all cosmic rays as free protons. Primary cosmic rays enter the atmosphere at high velocities in the range of 43% - 99.6% of the speed of light [7]. At standard temperature and pressure, primary cosmic rays in the atmosphere have an average interaction length of approximately 700 m, that is, they travel on average 700 m before interacting [8]. The interaction probability of primary cosmic rays can be taken to be directly proportional to the distance travelled through the medium [8].

Having entered the atmosphere, cosmic rays experience a various forces. Forces such as air resistance and gravity have little bearing on cosmic rays due to their small size and mass respectively [9][10]. The force which primarily dictates the change in motion of primary cosmic rays is the electronic stopping force quantified approximately by the Bethe formula [6]. The Bethe formula describes a force opposing the motion of cosmic ray particles due to their interactions with electrons in particles of the medium which they traverse [6]. The cosmic ray particles have positive charge and thus ionise atmospheric particles as they move past them; ionisation of these electrons requires energy, slowing the cosmic ray particle [6]. The slower the cosmic ray moves, the greater the density of ionisation events induced in atmospheric particles, hence the cosmic ray decelerates more rapidly as its velocity decreases due to the electronic stopping force increasing [11]. The point of maximum stopping force, known as the Bragg peak, occurs just before the particle slows to a complete stop [11]. This is displayed in the FIG 1.

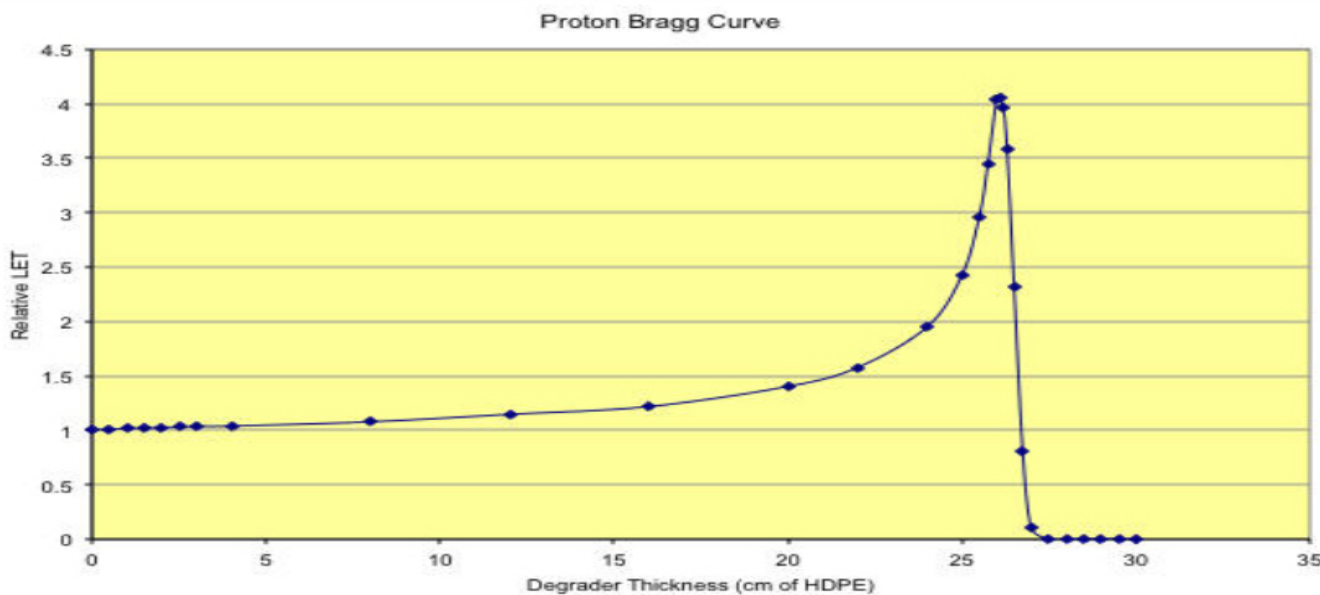


FIG. 1. A figure displaying the Linear Energy Transfer (LET) as a function of distance travelled through the medium for a 205 MeV proton travelling in High Density PolyEthylene (HDPE) [11]. The Bragg peak, the point of highest energy transfer to the HDPE, is clearly visible as the proton slows to a stop.

The Bethe formula was used in the model both in full and using a non-relativistic reduction; these are displayed the in Equations below [6].

$$-F = -\frac{dE}{dx} = \frac{4\pi n z^2}{m_e c^2 \beta^2} \left(\frac{e^2}{4\pi\epsilon_0} \right)^2 \ln \left(\frac{2m_e c^2 \beta^2}{I(1 - \beta^2)} - \beta^2 \right) \quad (1)$$

Equation 1 simplifies at non-relativistic speeds to Equation 2.

$$-F_{v \ll c} = -\frac{dE}{dx} = \frac{4\pi n z^2}{m_e v^2} \left(\frac{e^2}{4\pi\epsilon_0} \right)^2 \ln \left(\frac{2m_e v^2}{I} \right) \quad (2)$$

In the above formulae, F and $F_{v \ll c}$ are the stopping force acting on the particle, E is particle kinetic energy, x is the distance propagated by the particle in the medium, n is the electron number density, z is the particle charge relative to the electron charge magnitude, m_e is the electron mass, c is the speed of light in a vacuum, $\beta = \frac{v}{c}$ where v is the particle speed in the direction of propagation, e is the electron charge magnitude, ϵ_0 is the permittivity of a vacuum, I is the mean excitation potential of air. In the simulation, the value used for n was calculated for the electron density of the Mesosphere, this choice is further explained in Section III B. It can be seen that the equation does indeed produce a force by considering the particle as doing work to move through the atmosphere where energy is required to move against the electronic force acting on the particle; the equation for work is $dE = F dx$ hence $F = \frac{dE}{dx}$ [12]. The equation for work written is only valid in this form provided the force F acts parallel to the direction of displacement x [12].

These two equations form the basis of the simulation in that they represent the only force applied to the simulated particles. These equations are not vector equations, hence in the model, they are applied independently in each of the X, Y and Z axis directions. The simulation runs Equation 1 initially and transfers to Equation 2 when the particle drops below relativistic speeds in that component of the velocity vector. There is one clear limitation which is attributed to both equations, when the particle moves at speeds below a certain limit, the values within the natural logarithms is between zero and one; these values can never produce a negative number as the natural logarithm of a negative number is undefined for real numbers [13]. The natural logarithm of a number between zero and one is negative [13]. Hence, as the speed of the particle drops below a certain minimum value, the direction of the force produced by these equations changes. This minimum speed is clearly a breaking point in the equations and is accounted for in the model. Further details are given in Section III B; it is important to recognise that, due to the Bragg peak, the approximation that the particle's speed drops to zero instantly, once it hits the equation breaking point speed, is reasonable.

After the electronic stopping force, the second major component of the simulation of primary cosmic rays is their interactions with air molecules. It is these interactions which produce secondary cosmic rays [1]. In experimental observations, it is found that primary cosmic rays undergo multiple collisions, each with a variety of possible secondary cosmic ray products [14]. This is best illustrated by FIG 2 shown at the end of this section.

In FIG 2 one can see that the Incident Primary Proton goes on to cause a second interaction after the first; it's second trajectory is labelled with 'P'. This occurrence is due to the fact that the primary cosmic ray will lose only a fraction of its energy in each collision and so will collide and interact multiple times [14].

This phenomenon was not accounted for in the Python model. Instead the model implements a more ideal system where one hundred percent of the primary particles energy is lost when it collides. This decision was taken with the goal of more easily allowing the development of the simulation to include secondary cosmic rays where the secondary rays would inherit the final spatial and dynamic parameters of the primary cosmic rays as their initial parameters. This was not achieved within the time constraints of the project however, and the lack of multiple interactions for primary particles remains a clear limitation of the model.

As stated, primary have an average interaction length of 700 m [8]. This observation was used in the model to implement interaction probability by taking a Gaussian distribution weighted such that the average cosmic ray travels 700 m. Further details on the implementation of this interaction probability are given in Section III E.

The properties of the primary cosmic rays measured by the model include it's spatial and dynamic parameters as well as the particle total energy. Each of these are tracked over the run time of the simulation. Rather than looking to conserve physical quantities, the aim of the model is to reproduce relationships between the physical quantities

observed in real experiments. By design, the particles should lose energy as they travel. Hence particle total energy is not conserved. Energy loss as a function of distance travelled should produce a plot clearly displaying the Bragg peak [11]. Plotting the cosmic ray speed against time clearly show a steeper negative gradient as the particle slows down, demonstrating that slower particles do experience a greater electronic stopping force [6]. Finally, a figure showing the three dimensional trajectories of each particle should show that higher energy cosmic rays travel exponentially further into the atmosphere since they decelerate more slowly than lower energy cosmic rays. The average interaction length of cosmic rays on such a plot should be 700 m.

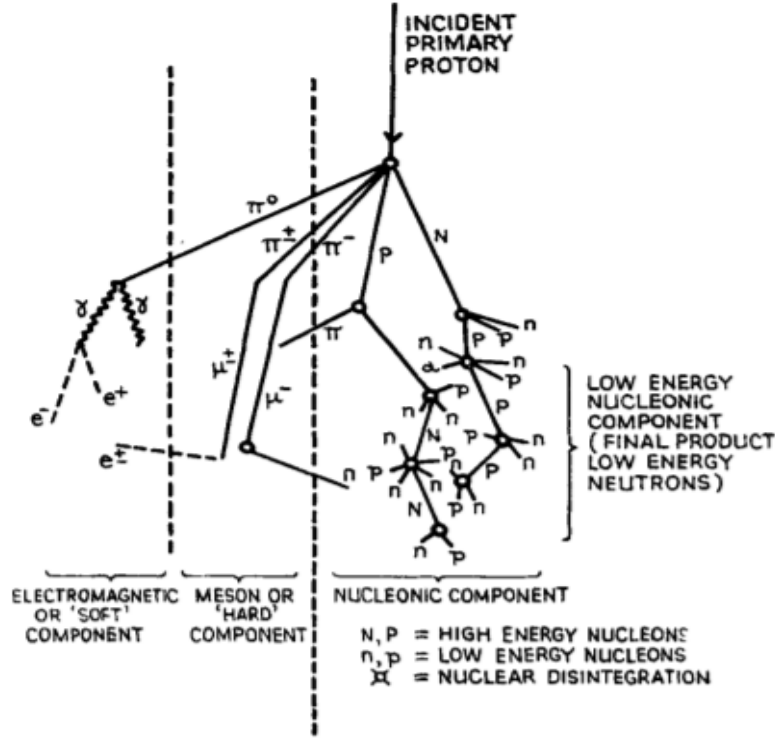


FIG. 2. A diagram illustrating how primary cosmic rays, incident on Earth's atmosphere, collide multiple times to produce secondary cosmic rays [14]. A variety of secondary products may be produced from each primary interaction.

III. DESIGN

As with any computer model, the simulation design went through a series of increasingly complex and more accurate iterations. Each of the major design milestones are detailed in the subsections below. Following this, the final design of the simulation is presented.

A. Creating Charged Particles

To initialise particles in the simulation, a simple particle class was written. This gave a position, velocity, acceleration, mass and name to each particle. It also contained key functions such as the ability to update the particle velocity and position using its acceleration and a time step through the Euler-Cromer method [15].

In order to experience an electronic stopping force however, a particle must have charge. Cosmic rays in the model are taken to be exclusively protons, which have a positive charge equivalent to the magnitude of the electron charge [16]. To include this parameter, an inheritance class was created. This allowed the initialisation of a proton with all the parameters defined by the particle class, as well as a charge parameter. This class is called **Charticle**.

Having created classes which initialise protons in three dimensional space, work to simulate the atmosphere through the forces it applies to the proton could begin.

B. Applying the Bethe Formula

As briefly outlined in Section II, the atmosphere in the simulation is defined by the electronic stopping force it applies on primary cosmic rays. Earth's atmosphere can be defined using distinct layers, as the first layer with a significant molecular density, in this model the Mesosphere is considered to be the first layer in which a significant stopping force is applied to the particle [5]. Below the Mesosphere is the Stratosphere followed by the Troposphere; these layers as well as their respective height ranges are shown in FIG 3 below.



FIG. 3. A diagram displaying the layers of the atmosphere and their respective height ranges [18]. The density of air in each layer is inversely proportional to its distance from Earth's surface.

At sea level, the air has a mean density of about $\langle \rho \rangle = 1.225 \text{ kg m}^{-3}$ and this density decreases by about fifty percent every 5.6 km [17]. Using this, one can calculate the mean densities of each of the three layers; these calculations are given in appendix A. The electronic stopping force of each layer is dependent on its mean density since Equations 1 and 2 are functions of electron number density of the medium. Hence, as the particle travels from a higher atmospheric layer to a lower one, the electronic stopping force experienced will increase irrespective of the particle dynamics.

The change in stopping force as the particles traverse the different layers would play a larger role if the simulation were extended to include secondary cosmic rays. However, even the fastest primary cosmic rays slow to a stop just after entering into the Stratosphere at a height of about 45 km above the Earth's surface. The electron number density

in the final simulation has simply been set to that of the Mesosphere multiplied by two. This increase accounts for the fact that higher energy cosmic rays do enter the increased density of the stratosphere and, in the actual physical system, this density increases as a gradient and is not a fixed value. The mean excitation potential of air is not a function of density and so has the same value in all atmospheric layers.

In the simulation code, the two iterations of the stopping force are applied hierarchical manor; if the cosmic ray speed drops below the relativistic threshold, taken to be $v = 0.033c = 1 \times 10^7 \text{ ms}^{-1}$, the applied force is calculated via Equation 2 rather than Equation 1. If the cosmic ray speed falls below $v = 0.0091c = 2.74 \times 10^6 \text{ ms}^{-1}$, the low speed limit before the two equations break as explained in Section II, the dynamic parameters of the cosmic ray are set to zero such that it stops instantly. The low speed limit is the minimum speed such that $\frac{2m_e v^2}{I} < 1$ which is the condition for the natural log in Equation 2 to become negative.

This allowed a particle travelling linearly to slow to a stop due to the electronic stopping force of the atmosphere. The model was then extended to execute this method in each of the X, Y and Z axis directions consecutively. This is important given that the stopping force reduces particle energy through doing work, so it must be defined as acting in the direction parallel to the direction of particle motion [12]. Since the dynamic vector parameters, velocity and acceleration, are defined in terms of their X, Y and Z components, the stopping force in each direction can be calculated and applied independently. FIG 4 displays how the stopping force, at each time interval in the simulation, is applied cosmic rays in the simulation at this stage.

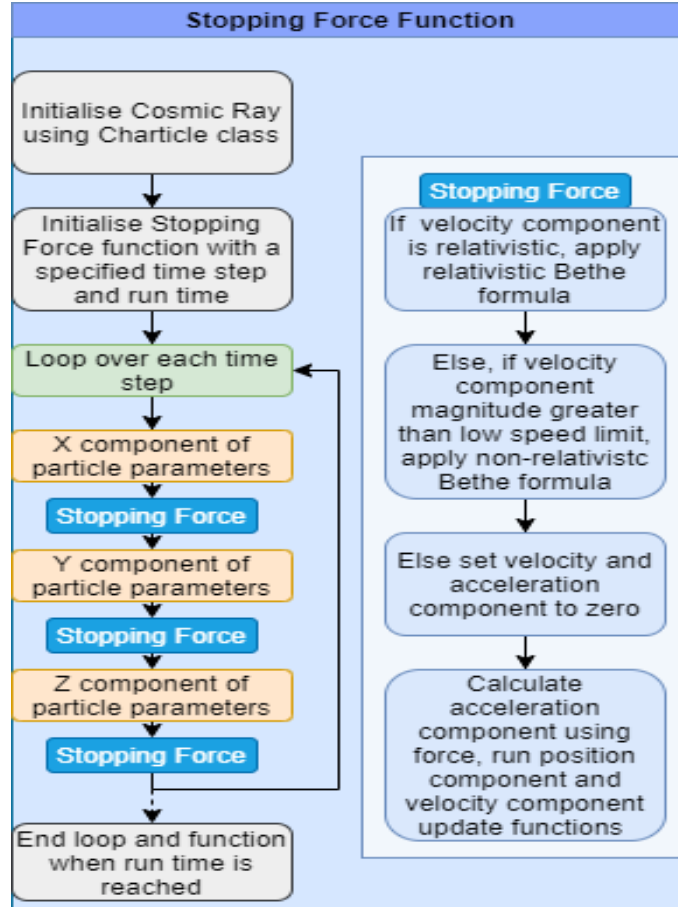


FIG. 4. A diagram displaying the process by which the electronic stopping force is applied to a single cosmic ray moving in the atmosphere for a given run time, t , where parameters are updated at each time step, Δt . In the simulation, the time step is a function of the run time, specifically, $\Delta t = \frac{t}{1000}$.

C. Utilising Data Frames

The primary cosmic rays have a number of parameters being updated and recorded throughout the simulation. It is important that each of these is updated correctly during the simulation making it imperative that cosmic ray parameter data is easy to access and display. For this reason, the **pandas** Python package was utilised to save particle data to a data frame.

A data frame is a two dimensional display using columns and rows to clearly present values in defined categories [19]. Data frames can be created in multiple ways. In this model, each of the parameters of the primary cosmic ray are updated and appended to a parameter list each time step during the simulation. These lists are then assembled as a dictionary, which is simply converted to a data frame using `DataFrame = pd.DataFrame(Dictionary)` where **pandas** is imported as **pd**.

This data frame is then pickled to be read in an analysis file. This allows figures to be generated easily by calling the desired columns from the particle's data frame to plot against each other. The data frame can also be printed in the terminal making it easy to see key values, such as the time step where the particle becomes stationary. Important plots include the trajectory of the particle in three dimensional space, the change in particle velocity over time and the energy lost by the particle to the electronic stopping force as a function of distance.

D. Multiple Particles

At the current iteration, the simulation consisted of a single particle experiencing the electronic stopping force in the atmosphere, where the variance in its parameters are recorded over time and can be easily accessed and analysed. Extending the simulation to include multiple particles proved reasonably simple in this particular simulation. This is because, unlike systems such as our solar system, where the motion of each body is dependent on the other bodies in the system, cosmic rays do not exert significant forces on each other provided they do not collide directly [20].

The first implementation method considered was to create a 'Bunch class' to initialise a group of cosmic rays for each simulation. This proved to be an unnecessary over complication however, given that the cosmic rays may be simulated independently. Instead, a function was created which generates a list of charged particle objects of length equal to a user input number of particles. The initial position and acceleration parameters of the particles are all the same, no initial acceleration and a position of $+8 \times 10^4$ m in the Y axis and zero in the X and Z axes. All cosmic rays are therefore initialised at the top of the Mesosphere [5]. The initial velocity vector is set as a function of the particle number and the total number of particles; this allows for two important conditions to be met. Firstly, the particles X and Z component velocities are functions of $\cos \theta$ and $\sin \theta$ respectively. $\theta \propto \frac{n}{N}$ where n is the cosmic ray number and N is the total number of cosmic rays in the group. this means cosmic rays will spread out in independent directions in the X-Z plane. The second condition, on the Y component velocity is shown in Equation 3 below.

$$v_Y = -(0.43 + 0.48 \frac{n}{N})c \quad (3)$$

n and N are again the particle number and total number of particles respectively, the values are chosen so that the magnitude of each cosmic ray's velocity lies in the range $0.43c$ to $0.996c$ where c is the speed of light in a vacuum. It is negative such that cosmic rays fall from the top of the atmosphere. This technique also ensures that within each bunch, irrespective of the number of particles, the cosmic rays have the maximum range of initial energies.

As stated, the cosmic rays do not exert any significant forces on each other during the simulation. For this reason, the program is designed such that it simulates each cosmic ray consecutively for the entire run time of the simulation, rather than simulating each cosmic ray before moving onto the next time step. This design choice increases the speed of the program and is valid only because the cosmic rays have no impact on each other. This process is visualised overleaf in FIG 5 which displays the atmosphere function used in the program.

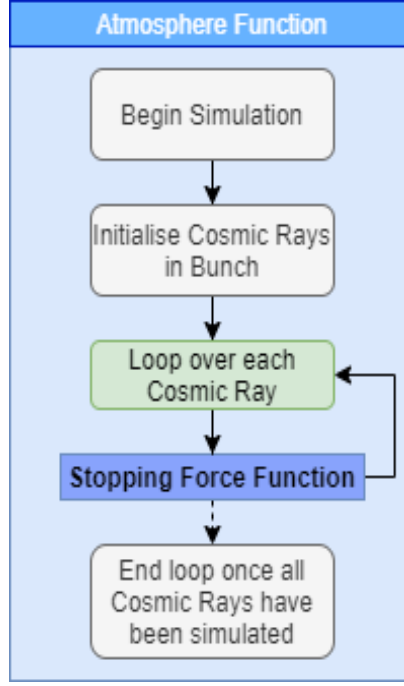


FIG. 5. A diagram displaying the process of simulating multiple cosmic rays where “Stopping Force Function” is the function given in FIG 4. The Atmosphere Function individually simulates each particle over the entire simulation run time before moving onto the next. This design is faster to run than updating all particles at each time step.

E. Primary Cosmic Ray Interactions

To allow for cosmic rays to interact, a second inheritance class was created. This class, the `CosmicRay` class, inherits the `Charticle` class detailed in Section III A. This class added three further parameters to the charged particles, `RestMass`, `Gamma` and `Interact`. `RestMass` is the initial mass of the cosmic ray and is constant, `Gamma` is the Lorentz factor due to vertical velocity, a function of velocity which becomes significant as a particle approaches the speed of light [21]. This is used to update the mass of the cosmic ray at each time step as relativistic particles increase in mass as their velocity nears the speed of light [21]. These two parameters are used to generate the relativistic energy of the particle and energy loss due to motion in the vertical direction. Since the large majority of each particle’s kinetic energy is in the vertical (Y-axis) direction, this is the direction focused on in analysis and thus most important to consider during the simulation. The `Interact` parameter is a value, initially set at zero, which indicates whether or not the cosmic ray has interacted. In the program, if `Interact` ≥ 50 the cosmic ray has interacted.

Primary cosmic ray interactions are outlined in Section II. The only quantitative information off which to base the simulation method is the mean interaction distance of primary cosmic rays, stated to be roughly 700 m. Combining this with the fact that interaction probability may be taken to be directly proportional to distance travelled through the medium, allows the use of a probability function weighted with respect to the distance travelled by the particle.

The program uses a Gaussian distribution with a standard deviation of -43 to 43 where the peak of the Gaussian distribution centres on zero. This means the majority of numbers generated will lie near zero with 68% of values within ± 43 with values beyond these possible, although rare [22]. This number is coefficient to the distance travelled by the particle divided by 700 m. The equation is shown in full in Equation 4.

$$I = g \frac{d}{700} \quad (4)$$

I is the value of `Interact`, a constant cosmic ray parameter with no units rounded to the nearest integer, g is the number generated using the Gaussian distribution and d is the distance travelled by the cosmic ray. In the simulation, the Gaussian distribution is set such that a particle is unlikely to interact immediately, but will quickly interact once the distance nears or surpasses 700 m.

Because the simulation runs independently in the X, Y and Z directions, the particle may interact due to motion in each of those directions. For this reason, the program checks to see if the particle will interact at the start of each time step such that an interaction does not occur after the particle has already had its parameters partially updated for a given time step. If any of the X, Y or Z interaction checks generate $I \geq 50$, the particle will be stopped immediately and marked as having interacted. Once the particle has interacted, the value of **Interact** is no longer updated.

When running the program, the user has the option to choose interacting or non-interacting cosmic rays. This is useful as one can see how the parameters change when cosmic rays can interact in an instant as well as when only the electronic stopping force acts on the cosmic rays.

F. Relativistic Adjustments

As explained in the section prior, relativistic mass as well as the Lorentz factor were included in the parameters of the particle in the **CosmicRay** inheritance class. These allowed for important values such as the total energy of the particle to be tracked over time.

A limitation of consecutively and independently updating values in the X, Y and Z directions is that the overall particle energy and speed, which are functions energy and velocity components in all three directions, are not updated properly. This issue occurs due to the low speed limit of Equations 1 and 2. As specified in Section III B, a velocity component will fall to zero when its magnitude drops below the low speed limit to avoid breaking the equations. This dropping to zero can be seen in the energy and speed of the particle as sudden drops in their value. These are clear to see when plotting these functions, making their plots redundant for analysis.

While the overall energy and speed are not accurately tracked, these values are in each independent direction. For this reason, the focus is chosen to be on the vertical (Y-axis) energy and speed as this is the direction with the majority of each particles energy. The particle Lorentz factor is therefore only calibrated using the Y-axis velocity and the values of particle energy due to vertical velocity and vertical speed are tracked through each time step of the simulation.

G. Test Functions

Test functions using **pytest** have been written and included in the program for each of the functions which return clearly testable results. Those that were not tested include functions which plot figures and the **Atmosphere** function which saves cosmic ray data to a data frame. Key tests included those of supporting functions which allow more complex functions to run. These must work as desired to ensure the accuracy of the simulation. Tests on the **CosmicRay** class functions were also written to ensure that the inherited parameters are being used as intended. Notable tests include checking that the function generating the bunch of cosmic rays initialises the correct number and gives these the correct initial parameters, checking that cosmic rays interact only when $I \geq 50$ and ensuring that cosmic ray energy is returning the correct value for a given Lorentz factor and particle mass.

H. Final Design

The final iteration of the program implements all of the above features as well as further design improvements. Many of the functions used are contained within support function files to improve the ease with which the code can be read and edited. It can simulate up to one thousand cosmic rays in a single simulation; more if the user is willing to wait for a longer time.

The final program runs entirely from the **RunSimulation.py** file which produces three figures, the three dimensional trajectory of the particles, the vertical velocity of the particles as a function of time and the vertical energy of the particles transferred to the atmosphere as a function of distance travelled. The run time is set so that the highest energy cosmic rays will just come to a stop if they do not interact. There is the option of printing the full data frame of any particles given when running the simulation. If the user chooses to have interacting cosmic rays, the program will also print the mean interaction distance of the cosmic rays as well as the number which interacted. The running process of the full simulation is displayed in Fig 6.



FIG. 6. A Diagram showing the process by which the simulation runs, in full. This builds on the diagrams shown in FIGS 4 & 5. The simulation is started by running the `RunSimulation.py` file in the terminal.

IV. RESULTS & ANALYSIS

The final iteration of the program produces a simulation of primary cosmic rays propagating in the upper atmosphere. While it would be of greater use if the model were extended further to include secondary cosmic rays, the results produced for primary cosmic rays reflect the physical observations to a reasonable accuracy.

A. Non-Interacting Primary Cosmic Rays

Section II details how primary cosmic rays experience an electronic stopping force which grows exponentially as the particles lose velocity during their propagation through the atmosphere. The simulation accurately produces these results and does not lose accuracy if a greater number of cosmic rays are simulated. This is shown in FIG 7 which shows the trajectory of non-interacting cosmic rays over the course of the simulation, for different numbers of simulated rays. FIG 8 shows the plot of the vertical velocities of cosmic rays over time, taken from the same simulations.

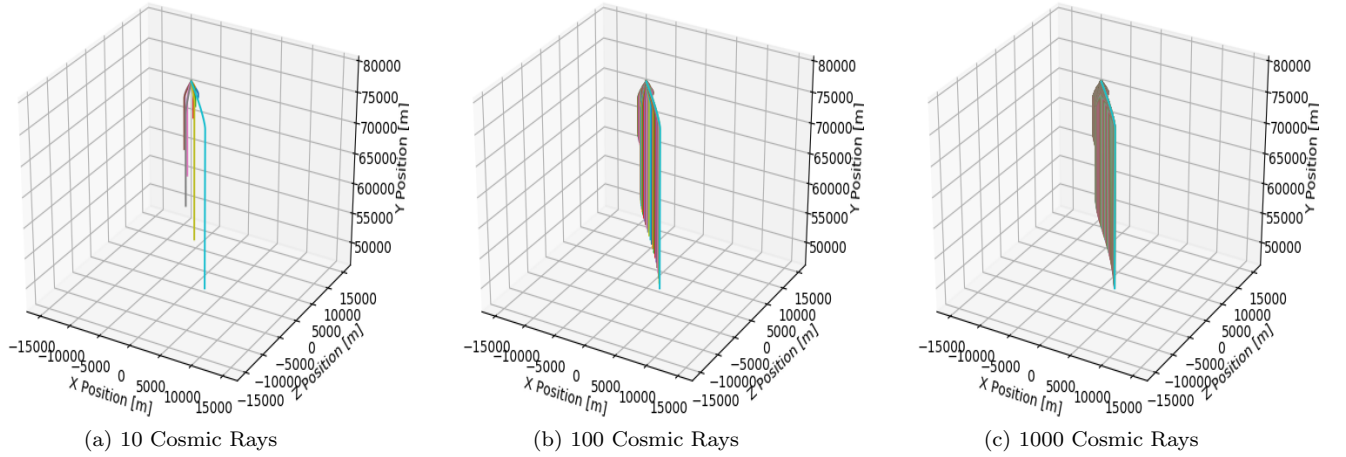


FIG. 7. Figures displaying the trajectory through the atmosphere of non-interacting cosmic rays, for simulations of 10, 100 and 1000 cosmic rays. Each coloured line is a single cosmic ray. The cosmic rays initialise at the top of the mesosphere and propagate downward into the atmosphere. Lower energy cosmic rays have exponentially shorter trajectories.

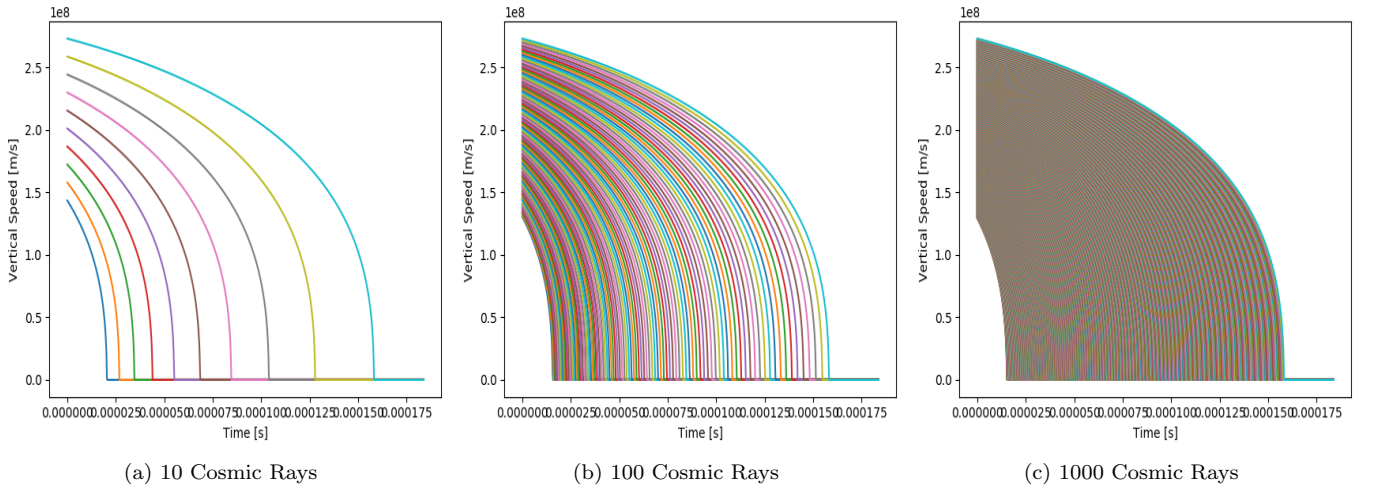


FIG. 8. Figures displaying the vertical speed as a function of time for non-interacting cosmic rays, for simulations of 10, 100 and 1000 cosmic rays. Each coloured line is a single cosmic ray. The cosmic rays initialise at their maximum speed and slow down due to the electronic stopping force applied by electrons in atmospheric molecules. The cosmic rays decelerate exponentially quicker over time.

These figures clearly display that the desired deceleration effect is occurring in the program. FIG 7 shows that higher energy cosmic rays travel exponentially further; this is because they decelerate more slowly. This is clearest in FIG 7(a) where the highest energy cosmic ray, blue line, has travelled further than the second highest energy cosmic ray, yellow line, by a greater distance than it travelled further than the third highest energy cosmic ray. That is to say, the distance between stopping points of consecutive cosmic rays increases with initial cosmic ray energy. FIG 8 supports this claim, showing a steeper deceleration gradient the slower a cosmic ray is travelling. The three dimensional plots are of greater use when the program is run as the user has the freedom to rotate and scale the plot as desired. The cosmic rays travel out in different directions in the X-Z plane by design, this allows individual cosmic rays to be viewed more easily.

The final figure produced by the program is the energy loss of the cosmic rays, in the vertical direction, as a function of their distance travelled through the atmosphere. As stated in section II one would expect this to produce a Bragg peak curve as the particle slows to a stop. The Bragg peak of each simulated cosmic ray can be clearly seen in FIG 9 which suggests the program well simulates non-interacting primary cosmic rays in each independent direction. Although, as stated in Section III F, this is not the case if one were to look at the overall energy loss as a function of distance or overall speed as a function of time.

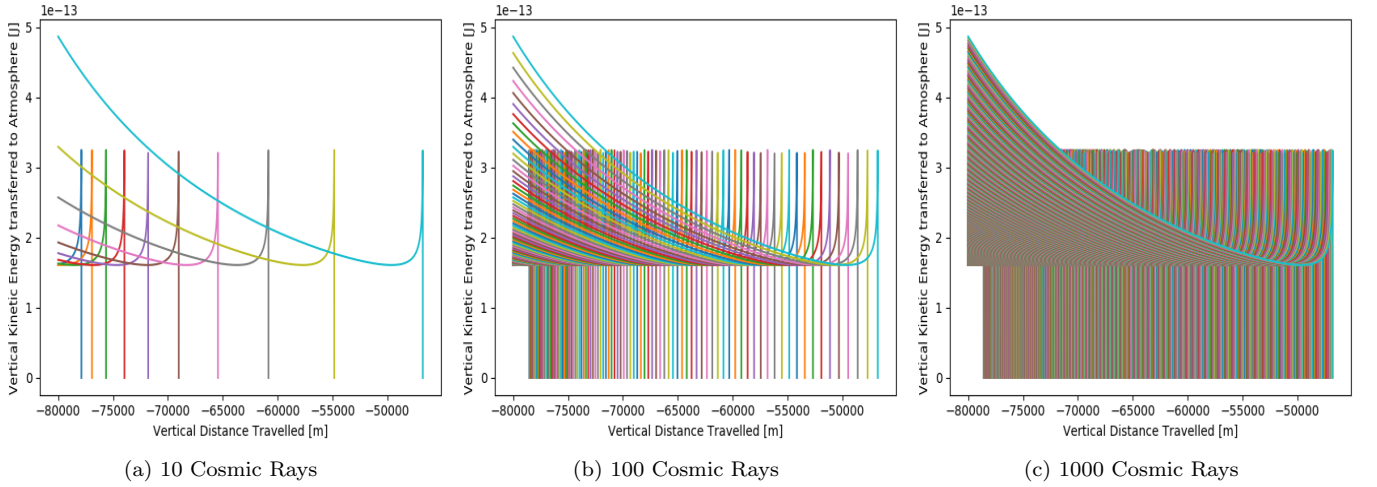


FIG. 9. Figures displaying the Y component energy transferred to the atmosphere as a function of distance travelled for non-interacting cosmic rays, for simulations of 10, 100 and 1000 cosmic rays. Each coloured line is a single cosmic ray. The cosmic rays initialise at their maximum energy and lose energy due to the electronic stopping force applied by electrons in atmospheric molecules. The energy loss peaks just as the cosmic rays come to a stop creating the phenomenon known as a Bragg peak [11].

Comparing FIGs 1 and 9, we see that the program clearly produces the Bragg peak effect, suggesting the simulation is working as intended. There are some clear differences however such as the fact that the energy loss in FIG 9 for high energy particles decreases as a function of distance prior increasing into the Bragg peak rather than starting as a constant and then increasing into the Bragg peak as in FIG 1. This discrepancy is most likely a result of using a time step method to update cosmic ray parameters. The time step is a constant value as specified in FIG 4. This means that faster moving particles will move further and thus transfer more energy per time step than slower moving particles. This creates the issue in question, where the more energy a cosmic ray is initialised with, the greater the initial energy loss as a function of distance; this of course runs contrary to the physical observations as stated. One potential solution to this discrepancy would be to institute a time step inversely proportional to velocity, that is, higher energy particles would be updated more frequently. The implementation of such a change would likely lead to a flat initial energy transfer as shown in FIG 1 as well as in the low energy particles of FIG 9.

Another notable issue in FIG 9 is the Bragg peaks reach different maximum values. This is seen most clearly in FIG 9(b). Since all cosmic rays are protons moving through the same medium, one would expect that, despite their initial energies being different, their Bragg peaks before stopping would be identical. This is not the case in the simulation likely due to the aforementioned low speed limit in Equations 1 and 2. As specified in Section III B, this was resolved by having particle velocity and acceleration drop to zero as soon as the particle falls below this limit. In the case of the energy loss however, this means that there is a wide range of final particle energies that, when updated, would correspond to the particle speed being some amount less than the low speed limit. This produces a range of final kinetic energy transfers in the form of Bragg peaks with different maximums as shown. A potential solution to this

issue would be the implementation of a further reduction to the Bethe formula with no low speed limit.

B. Interacting Primary Cosmic Rays

Primary cosmic rays propagating in the atmosphere have an interaction probability proportional to the distance travelled and have a mean interaction length of 700 m [8]. These observations were accurately reproduced by the program and are illustrated for four simulations each using 50 cosmic rays in FIG 10; unlike the non-interacting cosmic ray simulation, interacting cosmic rays do not produce the same results each time for a given number of cosmic rays. The program applies both the stopping force and variable interaction probability to interacting cosmic rays. Given cosmic rays usually interact after only a short distance, relative to the distances propagated in FIG 7, the effects of the electronic stopping force are comparatively small.

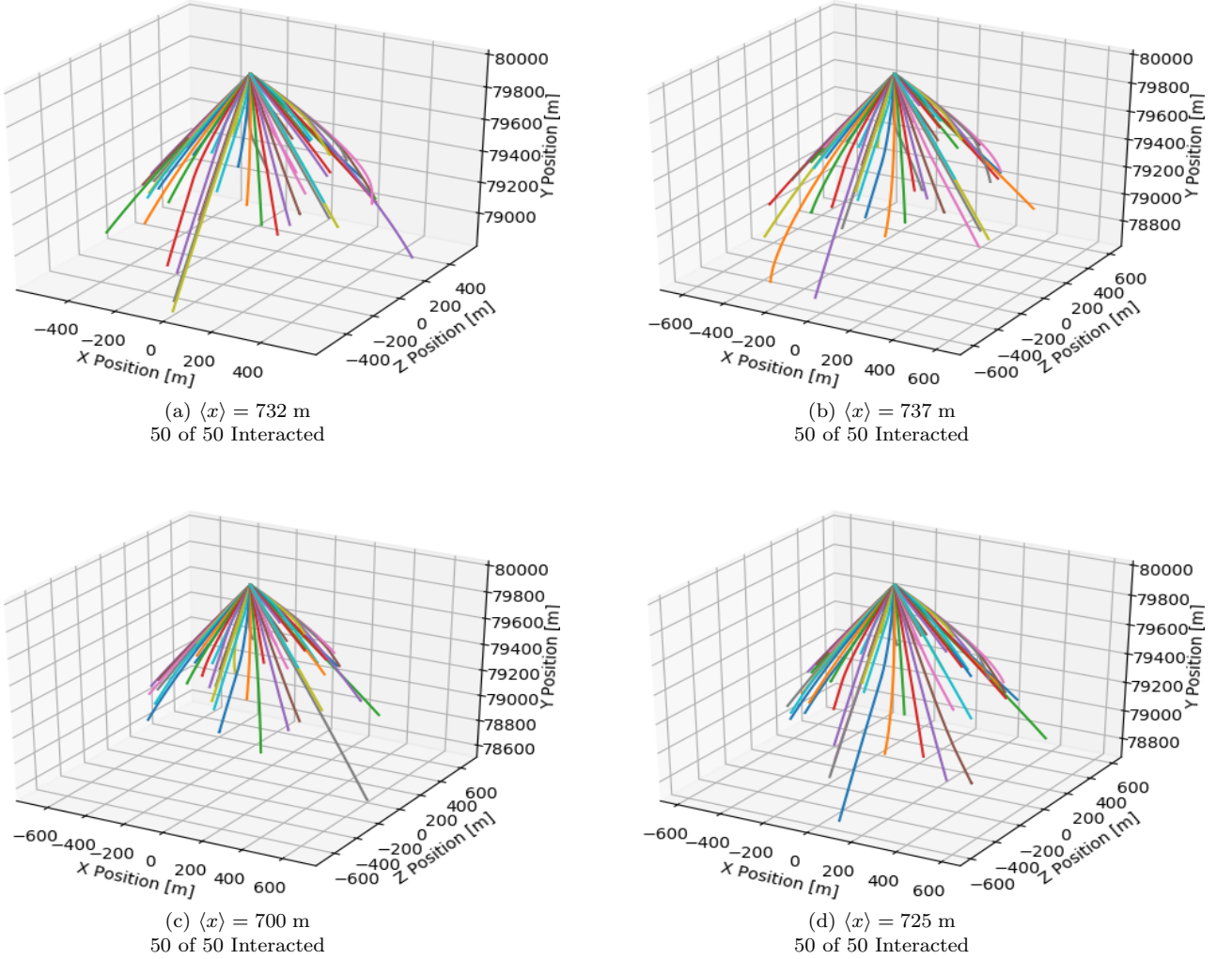


FIG. 10. Figures displaying the trajectory through the atmosphere of interacting cosmic rays, for four simulations of 50 cosmic rays. Each coloured line is a single cosmic ray. The cosmic rays initialise at the top of the mesosphere and propagate downward into the atmosphere. Each simulation produces a unique plot due to the random nature of interactions. $\langle x \rangle$ is the mean interaction length of cosmic rays in each simulation.

FIG 10 clearly shows that each simulation produces different results when interactions are enabled due to their random nature. The mean interaction lengths all lie near the desired value of 700 m, the average of the four being 723.5 m. This suggests that the Gaussian decay probability function is working reasonably well although a greater sample size of simulations would be required to assert that it produces the required mean interaction length. Also of

note is the fact that, in each simulation, all fifty particles interacted. This is the expected outcome given that the average cosmic ray is capable of travelling much further than 700 m, as shown in FIG 7, and interaction probability is proportional to distance travelled.

FIG 11 displays the vertical speed of interacting particles as a function of time in seconds. One can see that, initially, these are identical functions to those in FIG 8. However, they differ as the particle speed drops to zero the moment it interacts, as the particle itself no longer exists. As expected, the four graphs are unique as the results of each simulation are unique.

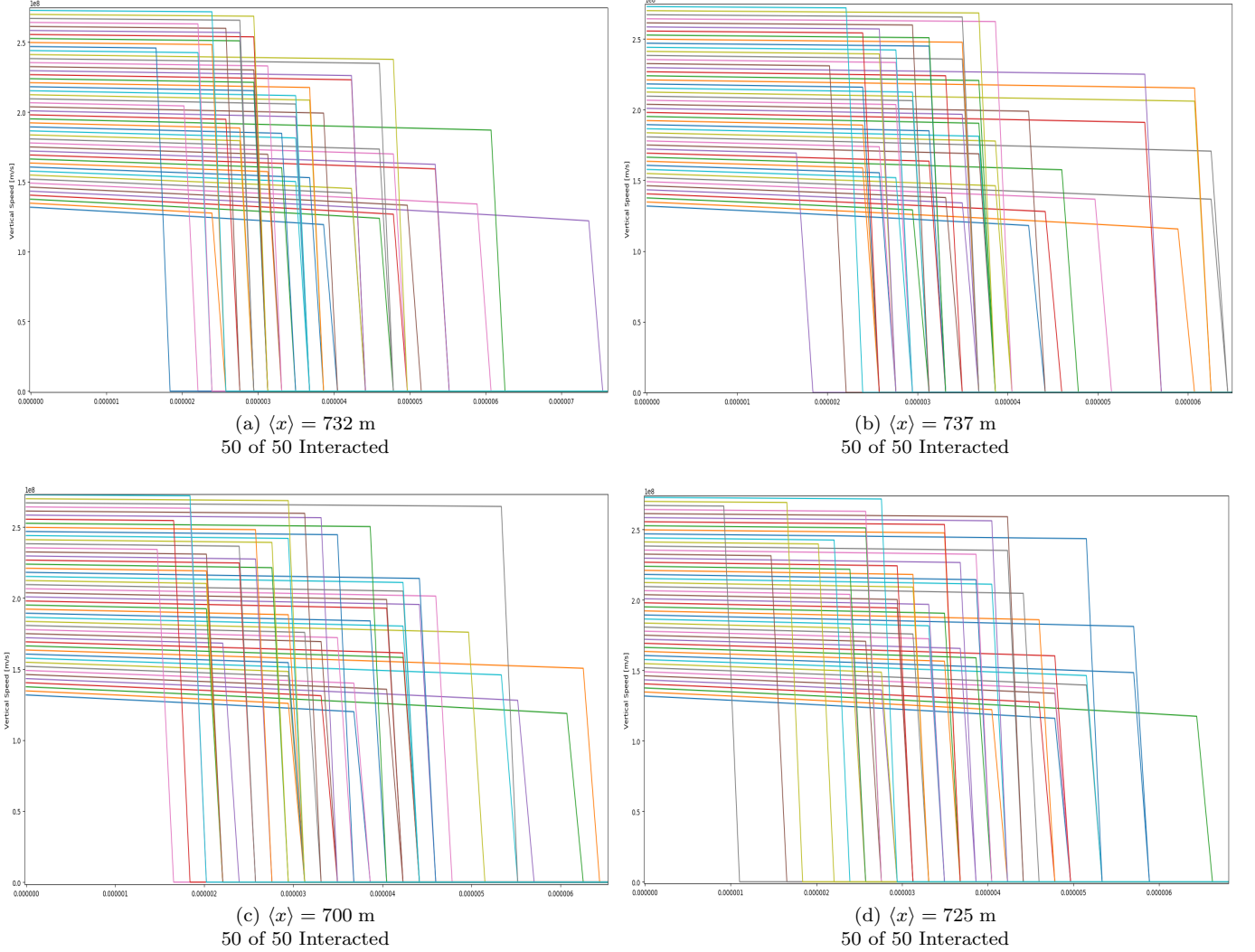


FIG. 11. Figures displaying the vertical speed as a function of time (seconds) for four simulations of 50 interacting cosmic rays. Each coloured line is a single cosmic ray. The cosmic rays initialise at their maximum speed and slow due to the electronic stopping force applied by electrons in atmospheric molecules. The speed does exponentially decrease, as in FIG 8, though all cosmic rays interact before this is clear to see. $\langle x \rangle$ is the mean interaction length of cosmic rays in each simulation.

The final figure for interacting cosmic rays, FIG 12, displays the vertical kinetic energy transferred to the atmosphere as a function of distance travelled by the particle. This graph differs greatly from its counterpart, FIG 9, which displays the same function for non interacting cosmic rays. Though not obviously apparent, the two graphs do in fact start identically; FIG 12 simply has a greater Y-axis scale. The initial energy transfer in FIG 9 is actually just above zero joules, on the order of 10^{-13} J as in FIG 9. This is not clear on the figure however given that the vast majority of energy transfer occurs when the cosmic ray interacts, each interaction is shown as a spike on the order of 10^{-10} J. Only after the particle interacts does the energy transfer drop to zero. Since it is assumed that the cosmic ray transfers all energy upon interacting, the Bragg peak phenomenon will not occur for a cosmic ray which interacts. As stated,

physical observations show that a primary cosmic ray may undergo multiple interaction collisions, each reducing it's kinetic energy; this is not included in the model and thus is a large limitation of it's accuracy.

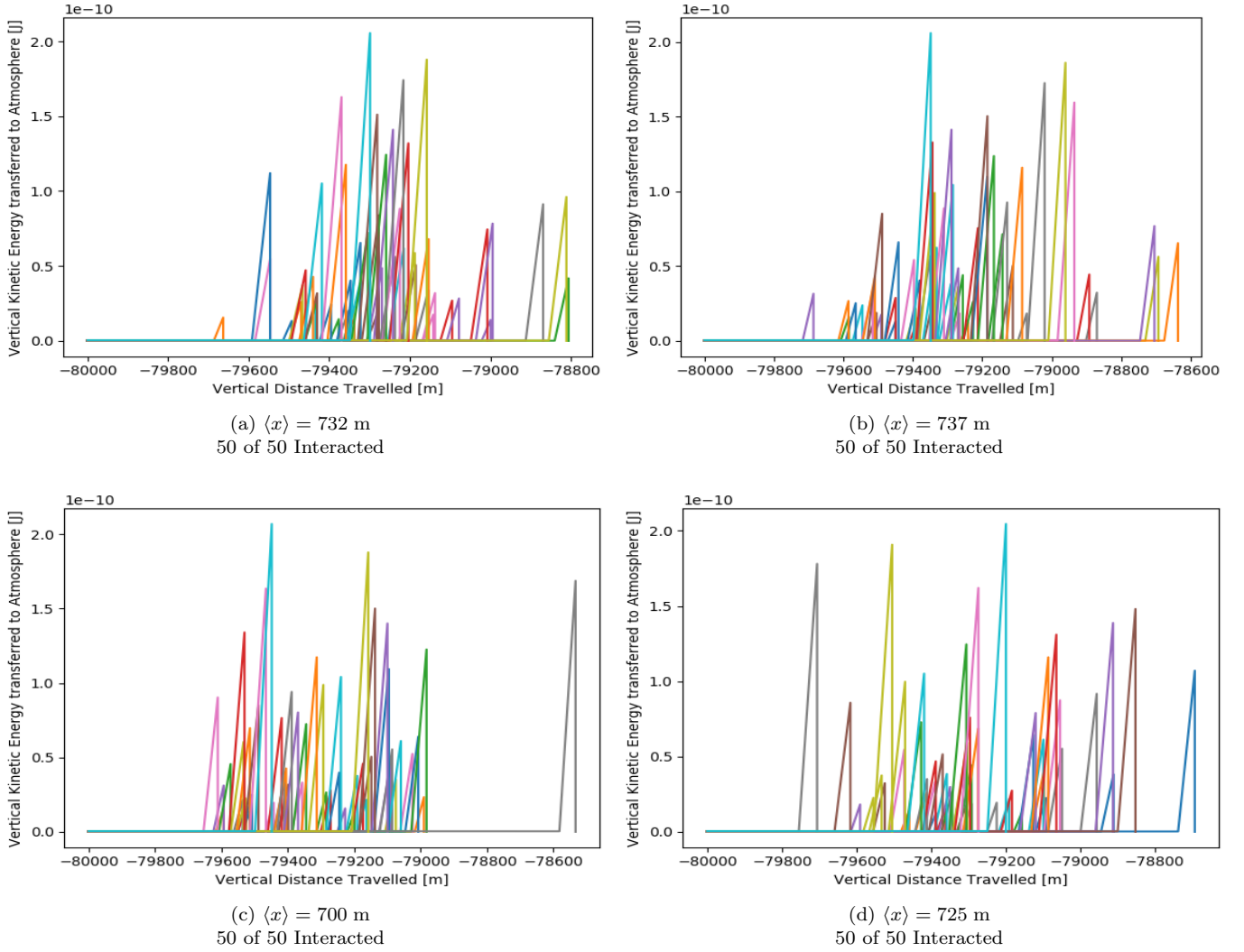


FIG. 12. Figures displaying the Y component energy transferred to the atmosphere as a function of distance travelled for four simulations of 50 interacting cosmic rays. Each coloured line is a single cosmic ray. The cosmic rays initialise at their maximum energy and lose energy due to the electronic stopping force applied by electrons in atmospheric molecules. This energy loss is negligible compared to the loss of all kinetic energy as the particle interacts; each spike on the graph is an interaction. $\langle x \rangle$ is the mean interaction length of cosmic rays in each simulation.

Overall, the program works reasonably well and produces the expected results. Limiting factors include the use of a constant time step as well as the simulation running totally independently in each of the X, Y and Z axis directions. The issue that the Bethe formula can only handle cosmic ray speeds down to a low limit velocity also reduces the accuracy of the Bragg peak in FIG 9.

V. FURTHER WORK

There are some clear limitations to the program which if corrected could greatly improve both its accuracy and application. The most obvious of these would be to implement secondary cosmic ray production and decay probability. While this would be the largest undertaking to achieve, including secondary cosmic rays would extend the model to include values that we can measure from Earth's surface, such as the secondary cosmic ray flux. What is more, the inclusion of secondary cosmic rays would allow for the visualisation of particle showers in a trajectory plot. To achieve this would require a large amount of work since the final parameters of the primary cosmic rays would need to be implemented as the initial parameters of the secondary cosmic rays. These secondary cosmic rays would then require decay probability functions that would occur after they had travelled for the duration of their mean lifetime as secondary cosmic rays are generally short lived. The decay probabilities would be weighted appropriately to allow for different secondary cosmic rays to be produced. The ideal conclusion of the project would be to measure the flux of secondary cosmic rays on Earth's surface generated by the simulation with the aim of replicating the values obtained by detectors in Lancaster Universities Particle Physics laboratory [23]

A second extension would be to alter the program so that the Bethe formula was implemented as a vector force so that the Stopping Force function, shown in FIG 4, is not required to run separately for the X, Y and Z axis directions. This would require the use of the β and v values as vectors in Equations 1 and 2 which may not be possible given one cannot take the natural log of a vector.

A final improvement would be the implementation of atmospheric density as a function of height above the Earth's surface in the Bethe formula. Though a small change, this would much more realistically represent the atmosphere as a physical system as it has a density gradient which increases as height decreases. The simulation currently runs with a constant density value.

VI. CONCLUSIONS

While the project was generally successful in simulating primary cosmic rays, the extension of the program to include secondary cosmic rays is key to improving the applications of the program as a model of a physical system. The program simulates primary cosmic rays from their entry into the Mesosphere to the point at which they interact with atmospheric particles or slow to a stop. The force opposing particle motion is the electronic stopping force of the atmosphere, calculated using the Bethe formula and interactions occur with a probability weighted using the mean interaction length of cosmic rays. The program can simulate any number of cosmic rays in reasonable time and does not decrease in accuracy if a greater number of cosmic rays are simulated.

The simulation produces cosmic rays which experience the electronic stopping force as desired such that a suitable Bragg peak is produced when measuring kinetic energy loss as a function of distance travelled; particle velocity as a function of time decreases exponentially as expected. When interactions are enabled, the mean interaction distance generally falls within 40 m of the desired value of 700 m. In each simulation, all simulated cosmic rays interacted which is the expected result. Due to how quickly cosmic rays interact, the interactions have much more impact on the results as the electronic stopping force is insignificant in the time frame within which the majority of cosmic rays will interact.

The program uses many of the advanced techniques required in the Phys 389 module and as such runs quickly and is simple to use as well as to read and edit. While improvements such as the use of a class in place of certain functions could improve the generalisation of the code, in its current state, it can be easily edited to simulate cosmic rays with various starting parameters moving through different mediums. Hence one could look at cosmic rays moving through different layers of the atmosphere or indeed different materials all together, provided the mean excitation potential and the electron density of the material are known. This level of flexibility in the program means that it could be used to simulate any particle experiencing the electronic stopping force of any medium, only requiring the initial parameters of the particle and stopping force functions to change. This is a clear success in the program design and vastly increases the applications of the model.

As stated, further additions to the program would prioritise the incorporation of secondary cosmic ray production and subsequent decay chains. The use of vector forces, if possible, would improve the analytical ability of the program and allow for more quantitative comparison to other models as well as physical observations. It would also be valuable to investigate the true ability of the model to simulate other systems dependent on electronic stopping power, such as the penetration of alpha particles into various materials such as lead. Modelling of this nature would have wide applications in various fields of physics.

VII. BIBLIOGRAPHY

- [1] Cosmic rays: particles from outer space. CERN. 2020. [online] available at: <https://home.cern/science/physics/cosmic-rays-particles-outer-space> [Accessed 19th March 2020]
- [2] What role do cosmic rays and solar activity play in climate change?. Physics at Lancaster University. 2014. [online] available at: <http://www.physics.lancs.ac.uk/news/002128/what-role-do-cosmic-rays-and-solar-activity-play-in-climate-change> [Accessed 19th March 2020]
- [3] Research Projects. Physics. Lancaster University. 2020 [online] available at: <https://www.lancaster.ac.uk/physics/study/projects/> [Accessed 19th March 2020]
- [4] Sinitsyna VG, Sinitsyna VY, Stozhkov YI. Red Dwarfs as Sources of Cosmic Rays and First Detection of TeV Gamma-rays from these stars. Journal of Physics: Conference Series:1181 01. 2018. [online] available at: <https://iopscience.iop.org/article/10.1088/1742-6596/1181/1/012018/pdf> [Accessed 19th March 2020]
- [5] Layers of Earth's Atmosphere. Centre for Science Education. 2015 [online] available at: <https://scied.ucar.edu/atmosphere-layers> [Accessed 19th March 2020]
- [6] Grimes DR, Warren DR, Partridge M. An approximate analytical solution of the Bethe equation for charged particles in the radiotherapeutic energy range. Nature. Scientific Reports 7. Article Number: 9781. 2017. [online] available at: <https://www.nature.com/articles/s41598-017-10554-0> [Accessed 20th March 2020]
- [7] Mewaldt RA. Cosmic Rays. California Institute of Technology. 1996.[online] available at: http://www.srl.caltech.edu/personnel/dick/cos_encyc.html [Accessed 20th March 2020]
- [8] Melissinos A C: Experiments in Modern Physics. Chapter 9: Cosmic Rays. 2018. [cited 20th March 2020] [Internet] Available at: <https://journals.aps.org/prd/abstract/10.1103/PhysRevD.98.030001>
- [9] Hall N. Size Effects on Drag. Glenn Research Center. NASA. 2015. [online] available at: <https://www.grc.nasa.gov/www/k-12/airplane/sized.html> [Accessed 20th March 2020]
- [10] Young HD, Freedman RA. University Physics with Modern Physics. 14th Edition. Ford AL, contributing author. Edinburgh Gate, Harlow, Essex, England: Pearson Education; 2016.[Chapter 13].
- [11] Bragg Curves and Peaks. NSRL User Guide III Technical Data. Brookhaven National Laboratory. NASA Space Radiation Laboratory. US Department of Energy. 2018.[online] available at: <https://www.bnl.gov/nsrl/userguide/bragg-curves-and-peaks.php> [Accessed 20th March 2020]
- [12] Work Equation. NWHS Physics Equations Page. Michigan State University. 2020[online] available at: https://msu.edu/~tuckeys1/highschool/physics/p_equations.htm [Accessed 23rd March 2020]
- [13] Logarithms. Algebraic Rules and Graphing. Atlas Project. University of Colorado. 2020.[online] available at: <http://lasp.colorado.edu/~bagenal/MATH/math82.html> [Accessed 20th March 2020]
- [14] Rochester GD. Cosmic rays and meteorology. Physics Department, University of Durham. Quarterly Journal of the Royal Meteorological Society. Vol 88, No. 378. 1962. [online] available at: <https://groups.physics.ox.ac.uk/climate/osprey/MJ/Roc62.pdf> [Accessed 22nd March 2020]
- [15] Nikolic BK. Euler-Cromer Method. Computational Methods of Physics. University of Delaware. 2018. [online] available at: http://www.physics.udel.edu/~bnikolic/teaching/phys660/numerical_ode/node2.html [Accessed 22nd March 2020]
- [16] Atomic structure and properties relating to bonding. BBC Bitesize. 2020. [online] available at: <https://www.bbc.co.uk/bitesize/guides/z9sdmp3/revision/2> [Accessed 22nd March 2020]
- [17] Lutgens FK, Tarbuck EJ. The Atmosphere: an introduction to meteorology. Englewood Cliffs, NJ: Prentice Hall. pp 14–17, ISBN 0-13-350612-6. 1995.
- [18] Atmosphere. Understanding Weather. Met Office. 2020. [online] available at: <https://www.metoffice.gov.uk/weather/learn-about/met-office-for-schools/other-content/other-resources/understanding-weather> [Accessed 23rd March 2020]
- [19] pandas.DataFrame. pandas. 2014. [online] available at: <https://pandas.pydata.org/pandas-docs/stable/reference/api/pandas.DataFrame.html> [Accessed 23rd March 2020]
- [20] Riebeck H. Planetary Motion: The History of an Idea That Launched the Scientific Revolution. EarthObservatory. Nasa. 2009. [online] available at: <https://earthobservatory.nasa.gov/features/OrbitsHistory> [Accessed 25th March 2020]
- [21] Young HD, Freedman RA. University Physics with Modern Physics. 14th Edition. Ford AL, contributing author. Edinburgh Gate, Harlow, Essex, England: Pearson Education; 2016.[Chapter 37].
- [22] Lacey M. The Normal Distribution. Statistical Topics. Department of Statistics and Data Science. Yale University. 1997. [online] available at: <http://www.stat.yale.edu/Courses/1997-98/101/normal.htm> [Accessed 25th March 2020]
- [23] Course Structure. Physics with Particle Physics and Cosmology MPhys Hons. Undergraduate Courses. Lancaster University. [online] available at: <https://www.lancaster.ac.uk/study/undergraduate/courses/physics-with-particle-physics-and-cosmology-mphys-hons-f373/#structure> [Accessed 25th March 2020]

Appendix A: Calculation of Mean Density for Atmospheric Layers

The three atmospheric layers relevant to the simulation are the Troposphere, Stratosphere and Mesosphere. This section details how the mean air density of each section was calculated, using the Mesosphere as an example given this is the layer through which primary cosmic rays propagate for the majority of their motion in the program.

Sea level air density is valued at $\langle \rho \rangle = 1.225 \text{ kgm}^{-3}$ and this density decreases by about fifty percent every 5.6 km [17]. The range of the Mesosphere is considered to be 50 – 80 km above sea level. As air density is inversely proportional to height above sea level, ρ_{max} occurs at $h_{min} = 50 \text{ km}$ and ρ_{min} occurs at $h_{max} = 80 \text{ km}$.

at ρ_{max} , $h_{min} = 50 \text{ km}$ the value of ρ_{max} is given by halving the sea level air density a number of times equal to h_{min} divided by 5.6 km

$$\frac{h_{min}}{5.6} = \frac{50}{5.6} = 8.929 \text{ [no units]}$$

ρ_{max} is therefore given by:

$$\rho_{max} = \frac{1.225}{2 \times 8.929} = 0.0686 \text{ kgm}^{-3}$$

likewise, at ρ_{min} , $h_{max} = 80 \text{ km}$,

$$\rho_{min} = \frac{1.225}{2} \times \frac{5.6}{80} = 0.0429 \text{ kgm}^{-3}$$

$\langle \rho \rangle$ for the Mesosphere is the average of these two:

$$\langle \rho \rangle = \frac{0.0686 + 0.0429}{2} = 0.0557 \text{ kgm}^{-3}$$

As specified in Section IIIB, to account for high energy cosmic rays reaching the Stratosphere and the fact that density in the atmosphere is in actuality a gradient, the value being used currently in the program is double this, That is:

$$\langle \rho \rangle = 0.111 \text{ kgm}^{-3} \text{ (3.s.f)}$$